A Unique Extraction of Metamaterial Parameters Based on Kramers–Kronig Relationship

Article *in* IEEE Transactions on Microwave Theory and Techniques · November 2010

DOI: 10.1109/TMTT.2010.2065310 · Source: IEEE Xplore

4 authors, including:

Zsolt Szabó
Budapest University of Technology and Economics
42 PUBLICATIONS **774** CITATIONS
SEE PROFILE

Ravi Sadananda Hegde
Indian Institute of Technology Gandhinagar
79 PUBLICATIONS **1,860** CITATIONS
SEE PROFILE

Er-Ping Li
Zhejiang University
381 PUBLICATIONS **5,132** CITATIONS
SEE PROFILE

A Unique Extraction of Metamaterial Parameters Based on Kramers–Kronig Relationship

Zsolt Szabó, Gi-Ho Park, Ravi Hedge, and Er-Ping Li, *Fellow, IEEE*

***Abstract*—In this paper, an improved algorithm for extracting the effective constitutive parameters of a metamaterial is derived. The procedure invokes the Kramers–Kronig relations to ensure the uniqueness of the solution. The accuracy of the method is demonstrated by retrieving the effective material parameters of a homogeneous slab. This study reveals under which conditions the calculation of the refractive index involves more than one branch of the complex logarithmic function. A metamaterial built up from wires and split-ring resonators is then investigated. The applicability and limits of the presented algorithm are explored by observing how the effective parameters of a metamaterial slab converge as its thickness is increased.**

***Index Terms*—Branching problem, effective material parameters, Kramers–Kronig relations, metamaterials.**

I. Introduction

ELECTROMAGNETIC metamaterial research [1]–[3] has attracted much interest over the last few years. In spite of considerable progress, researchers are still debating the fundamental issues and question the validity of the effective medium concept, which is essential for understanding the electromagnetic behavior of metamaterials (see [1, App. C] or [4]).

The usual design of metamaterials requires the computation of transmission-reflection data or S-parameters of a unit cell with a full-wave electromagnetic field solver. Electromagnetic material properties such as wave impedance, refractive index, electric permittivity, and magnetic permeability are then obtained by applying the effective medium theory [5], [6]. This theory replaces the electromagnetic response of the complicated metamaterial structure with the electromagnetic response of a homogeneous isotropic or anisotropic slab. The mathematical solution of this problem is generally not unique. To get a unique solution, physically justified constrains must be imposed. The continuity of complex electric permittivity and magnetic permeability with frequency must be enforced. Furthermore, a passive medium cannot have gain or lasing. At this point, it should be noted that, in this paper, the time–harmonic convention $\exp(-i\omega t)$ is used. Consequently, for passive media the imaginary part of the refractive index must be positive.

Several effective metamaterial parameter retrieval techniques are found in the literature [7]–[11]. In general, these methods yield a scalar electric permittivity and magnetic permeability, while the electromagnetic behavior of most metamaterial designs is anisotropic, requiring a tensor to properly describe it. Furthermore, a negative refractive index is only possible when the metamaterial is excited by a plane wave with specific polarization direction and angle of incidence. Even when all elements of the full permeability and permittivity tensor are determined [12], [13], the model can predict just the far-field behavior, while the near-field behavior of the metamaterial is lost. For most metamaterial devices, the coupling effects between the metamaterial and surrounding structures cannot be neglected. Hence, a full-wave simulation must be performed to obtain the correct electromagnetic fields.

In spite of these limitations, the effective material parameters can be useful in designing optimal metamaterial unit cells with a computer. Due to the high computational cost of the electromagnetic field solution, the metamaterial geometry can be optimized in a first design phase for a specific polarization and angle of incidence. For this purpose, a robust and fast effective metamaterial parameter retrieval procedure is required.

A method to retrieve the effective material parameters has been presented in [7]. The advantage of this algorithm is that the wave impedance and the imaginary part of the refractive index can be uniquely determined from the S-parameters. However, the retrieval algorithm has two limitations. In order to determine the real part of the refractive index, a cumbersome iterative method based on a Taylor series is required. In addition, when the usual passive material conditions $\mathrm{Im}(\epsilon) \geq 0$ and $\mathrm{Im}(\mu) \geq 0$ are imposed, the method cannot find any effective material parameters for some frequency regions. However, as it has been pointed out in [8] and [14] that the magnetic and electric dipoles induced in metamaterials are not independent of each other, and the passivity condition can be fulfilled even when $\mathrm{Im}(\epsilon) \leq 0$ or $\mathrm{Im}(\mu) \leq 0$. Relaxing this condition allows us to calculate effective parameters in regimes where the method in [7] fails.

The Kramers–Kronig integrals, which relate the real and imaginary parts of an analytic complex function, are fundamental physical relations based on the principle of causality [15], [16]. They were successfully applied to conventional optical materials [17]; for example, to calculate the refractive index from measured absorption data. In [18], it was shown that the Kramers–Kronig relations are valid for negative index materials as well.

Manuscript received October 25, 2009; revised June 20, 2010; accepted July 23, 2010. Date of publication September 07, 2010; date of current version October 13, 2010. This work was supported by the Agency for Science Technology and Research (A*STAR), Singapore, under Metamaterial Research Program Grant 0821410039.

The authors are with the Advanced Photonics and Plasmonics Research Group, Institute of High Performance Computing, Agency for Science Technology and Research (A*STAR), 138632 Singapore (e-mail: szaboz@ihpc.a-star.edu.sg; hegder@ihpc.a-star.edu.sg; parkgh@ihpc.a-star.edu.sg; eplee@ihpc.a-star.edu.sg).

Color versions of one or more of the figures in this paper are available online at http://ieeexplore.ieee.org.

Digital Object Identifier 10.1109/TMTT.2010.2065310

The purpose of this paper is to present an enhanced algorithm, which extracts the effective magnetic permeability and electric permittivity of a composite electromagnetic structure from calculated or measured transmission-reflection data. Such an algorithm will be instrumental in designing structures with optimized constitutive parameters. The novelty of our approach lies in employing the Kramers–Kronig relations to estimate the real part of the refractive index in order to ensure the uniqueness of the effective parameters.

The procedure of our algorithm is summarized in the following. The wave impedance can be uniquely determined from S-parameters. However, the calculation of the refractive index involves the evaluation of a complex logarithm. The complex logarithmic function is a multivalued function [19]. The resulting uncertainty is referred as a branching problem, which affects only the real part of the refractive index. To remove this ambiguity, the Kramers–Kronig relation can be applied to estimate the real part of the refractive index from the imaginary part. The physically realistic values of the refractive index are determined by selecting those branches of the logarithmic function that are closest to those predicted by the Kramers–Kronig relation. The algorithm also enforces the continuity of the refractive index versus frequency.

II. Effective Material Retrieval Algorithm With Kramers–Kronig Relations

The input data of the algorithm are the effective thickness d_{eff} and the complex S-parameters of the metamaterial slab calculated or measured at $\mathcal{N}$ distinct frequency points. As was shown in [7] and [8], for metamaterials with symmetrical geometry (in the direction of propagation of the electromagnetic wave), the effective thickness is just the sum of the length of the unit cells it contains. In this paper, metamaterials with symmetric geometries are considered. Therefore, no additional procedure is required to determine d_{eff}.

One way to generate the S-parameters of a metamaterial slab is to model it with a 3-D electromagnetic field solver. As we will show later, this algorithm is well suited to time-domain electromagnetic field solvers because large frequency ranges can be covered in a single run. However, in time-domain solutions, it is more difficult to control modes excited in the structure. When the observation points are placed in the near field of the periodic metamaterial structure, the unwanted higher order modes can be captured, which leads to wrong effective material parameter values. In order to obtain accurate S-parameters, the observation points should be positioned far enough from the surface of the metamaterial to sample only the dominant mode. Consequently, the phase delay caused by the additional distance must be compensated to determine the correct phase at the boundaries of the metamaterial.

As presented in [7], for a plane wave with normal incidence on a homogeneous slab, the wave impedance and the refractive index are related to the S-parameters as follows:

$$S_{11} = \frac{R_{01}(1 - e^{i2N_{\text{eff}}k_0 d_{\text{eff}}})}{1 - R_{01}^2 e^{i2N_{\text{eff}}k_0 d_{\text{eff}}}} \tag{1a}$$

$$S_{21} = \frac{(1 - R_{01}^2)e^{iN_{\text{eff}}k_0 d_{\text{eff}}}}{1 - R_{01}^2 e^{i2N_{\text{eff}}k_0 d_{\text{eff}}}} \tag{1b}$$

where $R_{01} = (Z_{\text{eff}} - 1)/(Z_{\text{eff}} + 1)$, $Z_{\text{eff}}(\omega)$ is the complex wave impedance, $N_{\text{eff}}(\omega) = n_{\text{eff}}(\omega) + i\kappa_{\text{eff}}(\omega)$ is the complex refractive index, n_{eff} is the refractive index, κ_{eff} is the extinction coefficient, k_0 is the free-space wavenumber, and ω is the angular frequency. From the previous relations,

$$Z_{\text{eff}} = \pm\sqrt{\frac{(1 + S_{11})^2 - S_{21}^2}{(1 - S_{11})^2 - S_{21}^2}} \tag{2}$$

$$e^{iN_{\text{eff}}k_0 d_{\text{eff}}} = \frac{S_{21}}{1 - S_{11}R_{01}}. \tag{3}$$

The sign of the wave impedance (2) is determined by imposing the conditions $\text{Re}(Z_{\text{eff}}) \geq 0$ and $\text{Im}(N_{\text{eff}}) \geq 0$, or equivalently, $\left|e^{iN_{\text{eff}}k_0 d_{\text{eff}}}\right| \leq 1$; for details, see [7] and [11]. The complex refractive index can be calculated as

$$N_{\text{eff}} = \frac{1}{k_0 d_{\text{eff}}}\{\text{Im}[\ln(e^{iN_{\text{eff}}k_0 d_{\text{eff}}})] + 2m\pi - i\text{Re}[\ln(e^{iN_{\text{eff}}k_0 d_{\text{eff}}})]\} \tag{4}$$

where m is an integer denoting the branch index. Separating the real and imaginary parts of the above expression, the refractive index and the extinction coefficient become

$$n_{\text{eff}} = \frac{\text{Im}[\ln(e^{iN_{\text{eff}}k_0 d_{\text{eff}}})]}{k_0 d_{\text{eff}}} + \frac{2m\pi}{k_0 d_{\text{eff}}} = n_{\text{eff}}^0 + \frac{2m\pi}{k_0 d_{\text{eff}}} \tag{5}$$

$$\kappa_{\text{eff}} = \frac{-\text{Re}[\ln(e^{iN_{\text{eff}}k_0 d_{\text{eff}}})]}{k_0 d_{\text{eff}}} \tag{6}$$

where n_{eff}^0 is the refractive index corresponding to the principal branch of the logarithmic function. The parameter extraction procedure takes advantage of the fact that the imaginary part of the refractive index is not affected by the branches of the logarithmic function. Therefore, it can be calculated from (6) without ambiguity. Knowing the imaginary part of the refractive index, we can determine the real part by applying the Kramers–Kronig relation

$$n^{\text{KK}}(\omega') = 1 + \frac{2}{\pi}\mathcal{P}\int_0^\infty \frac{\omega\kappa_{\text{eff}}(\omega)}{\omega^2 - \omega'^2}\text{d}\omega \tag{7}$$

where $\mathcal{P}$ denotes the principal value of the improper integral [16]. The limits of the integral are 0 and ∞, therefore the values of the S-parameters must be known for the entire frequency range. Since this is not possible, the integral must be truncated, and the Kramers–Kronig relations yield an approximation of the refractive index. For accuracy, the range of the integration should be as large as possible. Since time-domain methods yield the S-parameters over a large frequency range in a single run, they are particularly well suited to this algorithm. On the other hand, if the frequency becomes too large, we may reach a point where the concept of effective parameters is no longer meaningful since the guided wavelengths are on the order of the characteristic dimensions of the metamaterial structure.

The integration of (7) can be performed numerically by applying the trapezoidal rule of integration. To avoid the singularity of the improper Kramers–Kronig integral, the integration

is split in two parts (Cauchy method [20]), leading to the following approximation of the Kramers–Kronig relation:

$$\Psi_{i,j} = \frac{\omega_j \kappa_{\text{eff}}(\omega_j)}{\omega_j^2 - \omega_i^2} + \frac{\omega_{j+1} \kappa_{\text{eff}}(\omega_{j+1})}{\omega_{j+1}^2 - \omega_i^2}$$
$$n^{\text{KK}}(\omega_i) = 1 + \frac{\Delta\omega}{\pi}\left(\sum_{j=1}^{i-2} \Psi_{i,j} + \sum_{j=i+1}^{\mathcal{N}-1} \Psi_{i,j}\right). \quad (8)$$

Substituting the refractive index predicted by the Kramers–Kronig relation in (5), the branch number m can be expressed as

$$m = \text{Round}\left[\left(n^{\text{KK}} - n_{\text{eff}}^0\right)\frac{k_0 d_{\text{eff}}}{2\pi}\right] \quad (9)$$

where the function $\text{Round}()$ rounds towards the nearest integer. Therefore, the refractive index is calculated such that we select the branch that is closest to the value predicted by the Kramers–Kronig relation. The branch number m is substituted in (4), and the exact value of the refractive index is calculated. The algorithm then checks the continuity of the refractive index n_{eff}. A discontinuity close to the limit of the calculation zone may be caused by the truncation error in the Kramers–Kronig integral. If the discontinuity is far from the limits of the covered frequency range and the discontinuity perseveres even when the frequency interval of the simulation is increased, this indicates that the limit of the effective medium theory has been reached. Finally, by inverting the relations

$$N_{\text{eff}} = \sqrt{\epsilon_{\text{eff}}\mu_{\text{eff}}} \quad Z_{\text{eff}} = \sqrt{\frac{\mu_{\text{eff}}}{\epsilon_{\text{eff}}}} \quad (10)$$

the effective magnetic permeability and electric permittivity are calculated as

$$\mu_{\text{eff}} = N_{\text{eff}} Z_{\text{eff}} \quad \epsilon_{\text{eff}} = \frac{N_{\text{eff}}}{Z_{\text{eff}}}. \quad (11)$$

A code written in MATLAB,[1] which implements the presented algorithm, is available online.[2]

III. Origin of the Branching Problem and a Test of the Algorithm

In this section, the effective material parameters of two homogeneous metamaterial slabs are calculated. Both slabs have the same material parameters, but different thickness, namely, 40 and 200 nm.

The electric permittivity of many metamaterials can be represented by the Drude model

$$\epsilon_r(\omega) = \epsilon_\infty - \frac{\omega_p^2}{\omega^2 - i\gamma_c\omega} \quad (12)$$

where ϵ_∞ is the electric permittivity at high frequencies, ω_p is the Drude plasma frequency, and γ_c is the collision frequency; while the magnetic permeability can be described by the Lorentz model

$$\mu_r(\omega) = \mu_\infty - \frac{(\mu_s - \mu_\infty)\omega_0^2}{\omega_0^2 + i\omega\delta - \omega^2} \quad (13)$$

where μ_s is the static magnetic permeability, μ_∞ is the magnetic permeability at high frequencies, ω_0 is the magnetic resonant frequency, and δ is the magnetic damping factor. The parameters of the investigated homogeneous metamaterial slabs are $\epsilon_\infty = 1.8$, $\omega_p = 2\pi \times 0.8 \cdot 10^{15}$ rad/s, $\gamma_c = 80 \cdot 10^{12}$ rad/s, $\mu_s = 1.3$, $\mu_\infty = 1.1$, $\omega_0 = 2\pi \times 0.4 \cdot 10^{15}$ rad/s, and $\delta = 0.05 \cdot 10^{15}$ rad/s.

Once the thickness of the homogeneous slab is fixed and the material parameters are known, we can apply the analytical expressions (1a) and (1b) to calculate the S-parameters. The effective material parameter extraction algorithm is then employed to calculate the effective magnetic permeability and the effective electric permittivity. We compare the extracted material parameters to the exact values provided by the Lorentz and Drude models. The purpose of this comparison is to demonstrate the applicability of the algorithm and to estimate the accuracy of the extracted effective material parameters. This study also reveals under which conditions the calculations involve more than one branch of the complex logarithmic function.

Fig. 1(a) and (b) presents the S-parameters of the 40-nm-thick homogeneous slab, and Fig. 1(c) shows the refractive index for this case. In all the figures showing the complex refractive index N_{eff}, the imaginary part κ_{eff} is represented with point markers. The Kramers–Kronig approximation of the refractive index n^{KK} is plotted with circle markers. Possible branches of the refractive index n_{eff} for $m = [-3, 3]$ are plotted as well with upward-pointing triangle, asterisk, downward-pointing triangle, diamond, cross, and bold plus sign markers. The extracted refractive index n_{eff} is plotted with plus sign markers. The slab of 40 nm is thin compared to the wavelengths at which the refractive index is negative. In this case, the phase of S_{21} is continuous in the $[-180^\circ, 180^\circ]$ interval [see Fig. 1(b)]; consequently, no branching problem occurs. The real part of the refractive index calculated with the Kramers–Kronig relation exactly follows the branch corresponding to $m = 0$. The extracted effective electric permittivity and magnetic permeability are presented in Fig. 2. The inset shows the effective parameters in the double-negative frequency region.

Fig. 3 shows the S-parameters of the 200-nm-thick homogeneous slab. In this case, the phase of S_{21} presents several discontinuities, as can be seen in Fig. 3(b). This fact indicates that the 200-nm slab is thick compared to the wavelengths at which left-handed behavior occurs, and that there are several branches contributing to the physically correct refractive index, as can be seen in Fig. 4(a). Fig. 4(b) shows the branch number m as a function of frequency. In case of the thick slab, the branch number m can equal -2, -1, 0, and 1. Fig. 4(c) brings into focus the double-negative frequency region to relay the fine details of the negative refractive index and to show how the transitions from one branch to another occur.

[1][Online]. Available: www.mathworks.com/products/matlab/

[2][Online]. Available: http://effmetamatparam.sourceforge.net/

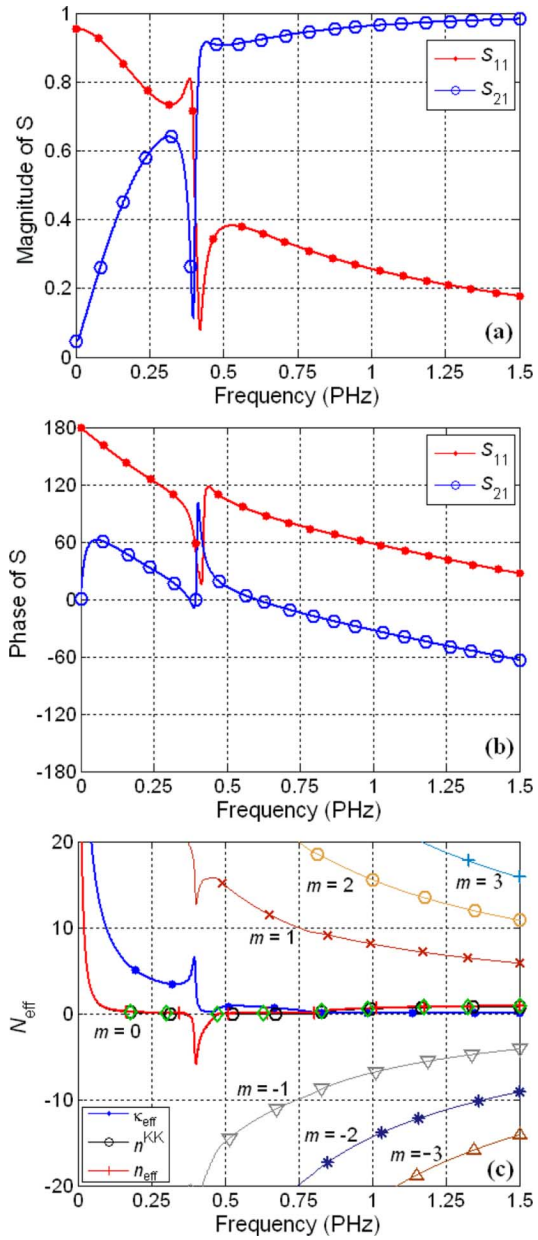

Fig. 1. S-parameters and the refractive index of the 40-nm-thick homogeneous slab. In (a), the magnitude, and in (b), the phase of the S-parameters are plotted. In (c), the calculated extinction coefficient κ_{eff}, the Kramers–Kronig approximation n^{KK}, several possible branches of the refractive index for $m = [-3, 3]$, and the extracted refractive index n_{eff} are presented. In this case, the refractive index follows the branch with $m = 0$. Note that 1 pHz $= 10^6$ GHz.

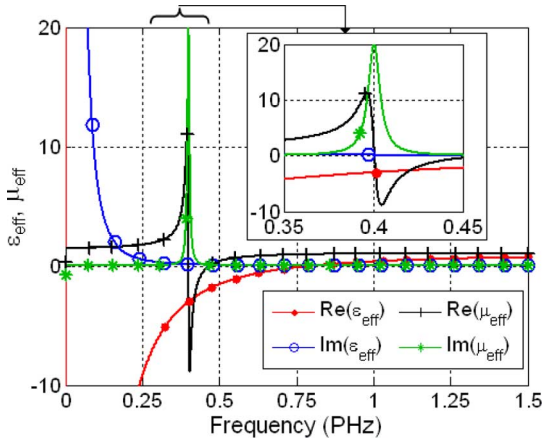

Fig. 2. Extracted effective electric permittivity and magnetic permeability. The inset shows the effective parameters in the double-negative frequency region. Note that the effective parameters are independent of the thickness of the homogeneous slab.

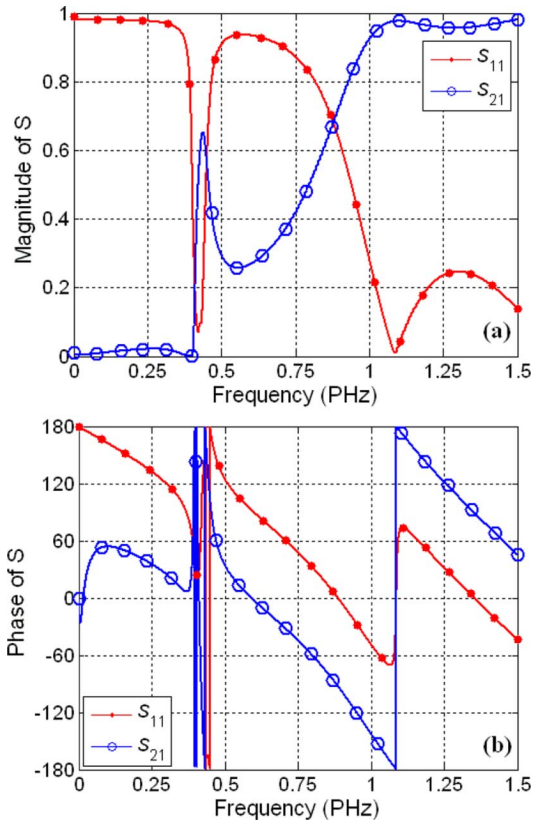

Fig. 3. (a) Magnitude and (b) phase of S-parameters for the 200-nm-thick homogeneous slab.

From Figs. 1(c) and 4(a), we can observe that the curves of the Kramers–Kronig approximation and of the refractive index exactly overlap. This fact indicates the accuracy of the approximation given by (8). The extracted electric permittivity and magnetic permeability are independent of the slab thickness. They are the same for both the 40- and 200-nm-thick slabs and equal the exact values given by (12) and (13). This indicates that the extracting procedure accurately reproduces the original values of ϵ_{eff} and μ_{eff} entered in the model of the metamaterial, and thus validates the proposed approach.

The phase of S_{21} yields useful information on several facts. If the phase change exceeds 180°, then more than one branch of the logarithmic function can contribute to the refractive index. In addition, it can also indicate the frequency range in which the refractive index can be negative. Comparison of Fig. 1(b) and (c) or Figs. 3(b) and 4(a) reveals that whenever the refractive index becomes negative, the slope of the phase S_{21} changes sign. However, a sign change in the slope of S_{21} does not necessarily imply negative refractive index, but it may indicate such an occurrence. This can be explained by the opposite orientation of the group and the phase velocity in the double-negative region [2].

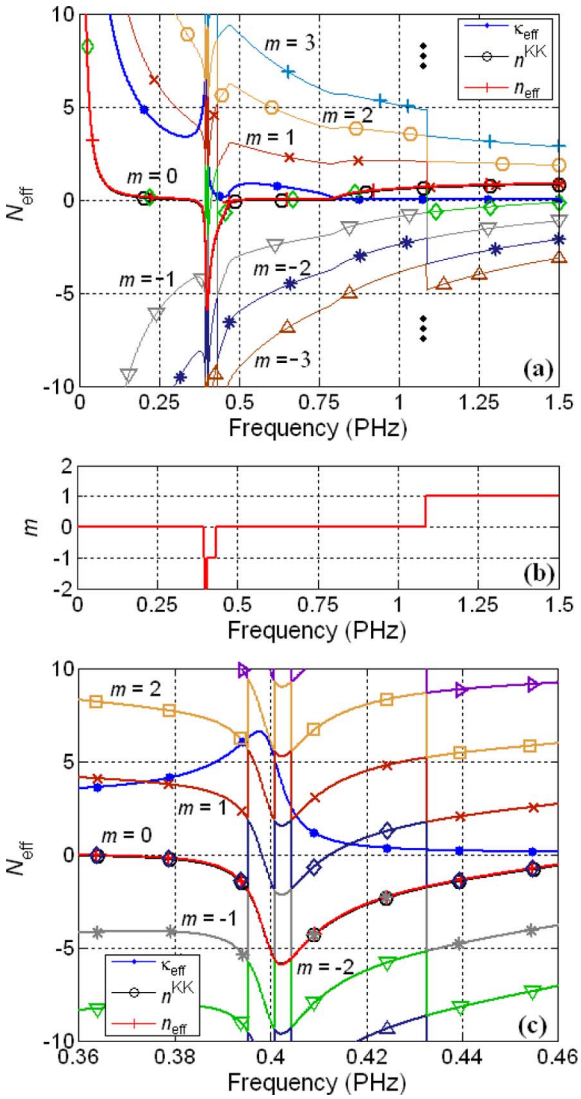

Fig. 4. (a) Refractive index of the 200-nm-thick homogeneous slab, (b) the branch number m, and (c) a zoom to the double-negative frequency region where more than one branch contributes to the refractive index. (a) presents the calculated extinction coefficient $\kappa_{\rm eff}$, the Kramers–Kronig approximation $n^{\rm KK}$, several possible branches of the refractive index for $m = [-3, 3]$, and the extracted refractive index $n_{\rm eff}$. Note that, in this case, the refractive index follows different branches of the logarithmic function.

IV. Effective Material Parameters of a Metamaterial Slab Consisting of Wires and Split-Ring Resonators

In order to demonstrate the effective parameter retrieval algorithm for a real metamaterial, a well-studied structure consisting of split-ring resonators and metallic wires is considered (see Fig. 5). The geometry of the unit cell, dimensions, and material parameters are the same as in [8]. In this metamaterial design, the role of the split-ring resonators is to provide the negative magnetic response, while the wires are responsible for producing the negative electric permittivity. This metamaterial design has been extensively discussed in literature, e.g., see [1, Ch. 4] or [21].

In our numerical simulations, the metamaterial is periodic in the direction perpendicular to the propagation of the electromagnetic wave, and the electric field is polarized parallel to the wires. At the same time, we consider metamaterials with one, three, five, or seven layers of unit cells in the direction of propagation. The aim of the calculation is to determine the effective parameters of this metamaterial in the frequency range from 5 to 20 GHz. Simulations show that this metamaterial presents many resonances outside of this frequency range. Therefore, to get a good estimate for the Kramers–Kronig integral, the simulations cover the 0–30-GHz frequency interval. We found that when this frequency interval is even larger, the accuracy of the Kramers–Kronig approximation does not change noticeably. Note that the calculation of the S-parameters presented in this section was performed with the time-domain solver of the commercial software CST Microwave Studio.[3]

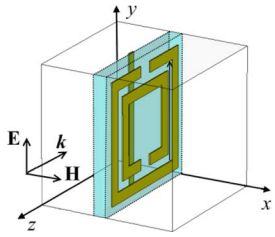

Fig. 5. Unit cell of the metamaterial slab composed of metallic split-ring resonators and wires separated by dielectric. Note that we consider a plane-wave excitation with perpendicular incidence, and an electric field polarized parallel to the wires.

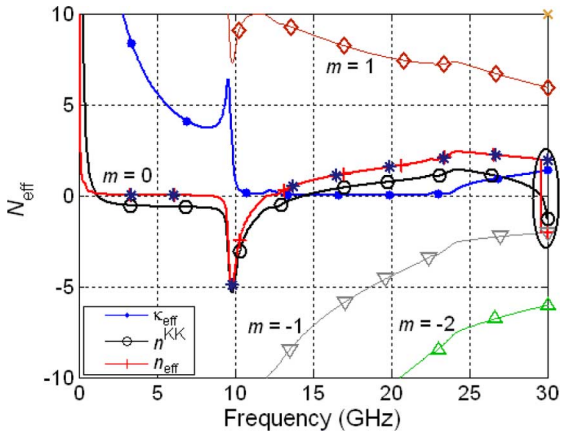

Fig. 6. Retrieved refractive index, extinction coefficient, the Kramers–Kronig approximation, and several branches of the only one-unit-cell-thick metamaterial slab. The refractive index has a discontinuity in the circled frequency region, but this is a numerical error due to the truncation of the Kramers–Kronig integral and can be removed by increasing the frequency range of the simulation.

The retrieved refractive indices and extinction coefficients are presented in Figs. 6–9, while Fig. 10 summarizes the effective electric permittivity and magnetic permeability in the frequency region of the first resonance, where the double-negative behavior occurs. As shown in Fig. 6, the metamaterial slab that is only one unit cell thick is thin compared to the wavelength in the considered frequency range. The calculated S-parameters are the same as in [8]. The phase of S_{21} is continuous on the $[-180^\circ, 180^\circ]$ interval. Therefore, the refractive index follows the zero branch (see Fig. 6). The discontinuity of the refractive index $n_{\rm eff}$ at the end of the covered frequency interval, marked in Fig. 6 by a circle, is a numerical error due to the truncation

[3][Online]. Available: www.cst.com

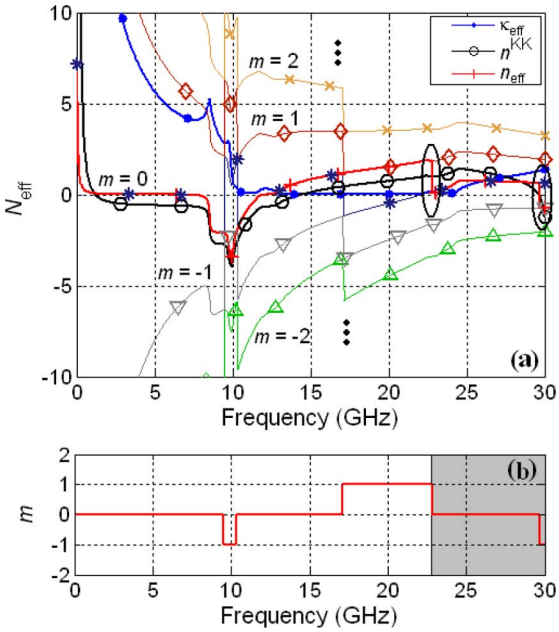

Fig. 7. (a) Retrieved refractive index $n_{\rm eff}$ and extinction coefficient $\kappa_{\rm eff}$ and (b) the branch number m of the three-unit-cell-thick metamaterial slab. In (a), the Kramers–Kronig approximation of the refractive index $n^{\rm KK}$ and several branches are plotted as well. The refractive index has discontinuity in the circled frequency regions. Note that the effective medium theory can be applied outside of the gray frequency region of (b).

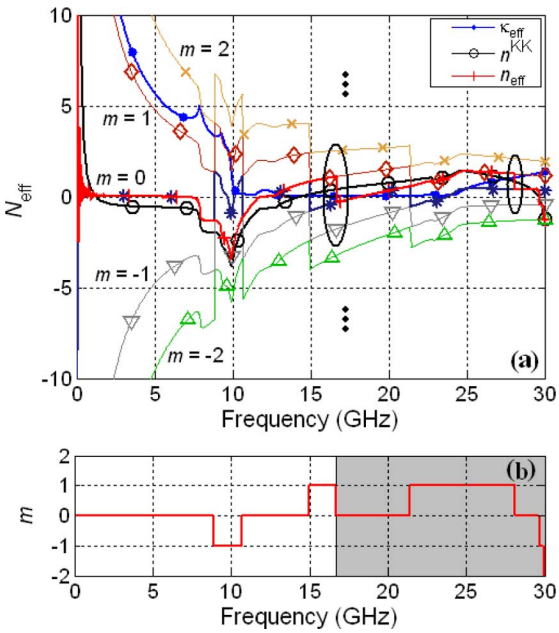

Fig. 8. (a) Retrieved refractive index $n_{\rm eff}$ and extinction coefficient $\kappa_{\rm eff}$ and (b) the branch number m of the five-unit-cell-thick metamaterial slab. In (a), the Kramers–Kronig approximation of the refractive index $n^{\rm KK}$ and several branches are plotted as well. The refractive index has discontinuity in the circled frequency regions. Note that the effective medium theory can be applied outside of the gray frequency region in (b).

of the Kramers–Kronig integral, and it can be removed by increasing the frequency range of the calculation. Note that in the following graphs presenting the refractive index, the circled regions correspond to frequency regions where a discontinuity of

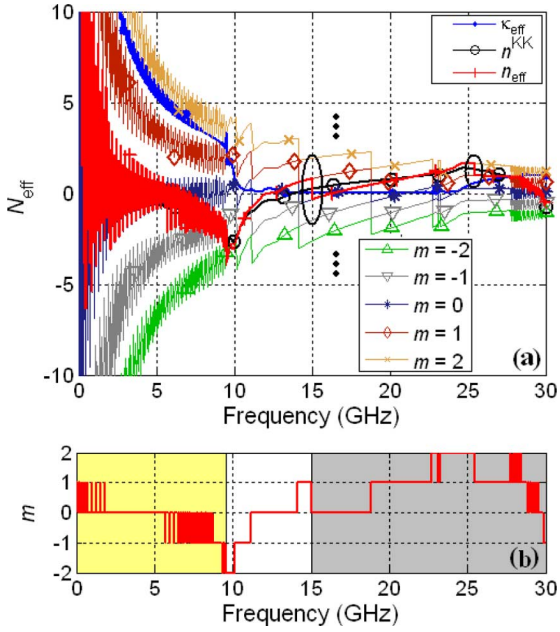

Fig. 9. (a) Retrieved refractive index $n_{\rm eff}$ and extinction coefficient $\kappa_{\rm eff}$ and (b) the branch number m of the seven-unit-cell-thick metamaterial slab. At low frequencies, the phase of the S-parameters is not well defined, leading to unphysical oscillations in the extracted metamaterial parameters. It is difficult to judge the validity of the effective parameters even in the frequency region between 10–15 GHz.

the refractive index occurs. The extracted effective material parameters are similar to those presented in [8].

The effective refractive index of a metamaterial with a thickness of three unit cells is presented in Fig. 7. This metamaterial is thick compared to the wavelength in the negative refractive index region. The calculations reveal that, in the double negative zone, the refractive index follows branches 0 and 1 [see Fig. 7(a) and (b)]. The refractive index has a first discontinuity at $f = 22.83$ GHz; this correspond to the first circled region in Fig. 7(a), and we found that this discontinuity cannot be removed by extending the frequency range of the simulation. By inspecting the possible branches around the discontinuity point, we note that branch $m = 1$ should be followed henceforth to enforce the continuity of the refractive index $n_{\rm eff}$. It should be noted that the algorithm proposed in [7] also fails in this region. Following the branch $m = 1$ from the discontinuity point until the end of the considered frequency region, the imaginary part of the electric permittivity or the imaginary part of the magnetic permeability are alternatively negative. At the discontinuity point, the refractive index is $n = 1.85$ and the optical wavelength can be calculated as $\lambda_{\rm opt} = c_0/(nf) = 7.1 \times 10^{-3}$ m. The effective thickness is $d_{\rm eff} = 7.5 \times 10^{-3}$ m, which is comparable to the optical wavelength $d_{\rm eff}/\lambda_{\rm opt} = 1.05$. Therefore, we interpret this discontinuity as an upper limit of the effective medium theory. The gray areas in Fig. 7(b) represents frequency regions above this upper limit.

Fig. 8 refers to a metamaterial consisting of five layers of unit cells. Inspecting the continuity of $n_{\rm eff}$, we see that the location of the first discontinuity shifts to the lower frequency $f = 16.71$ GHz. In this case, the refractive index at the discontinuity is $n = 1.1$. The effective thickness of the metamaterial is

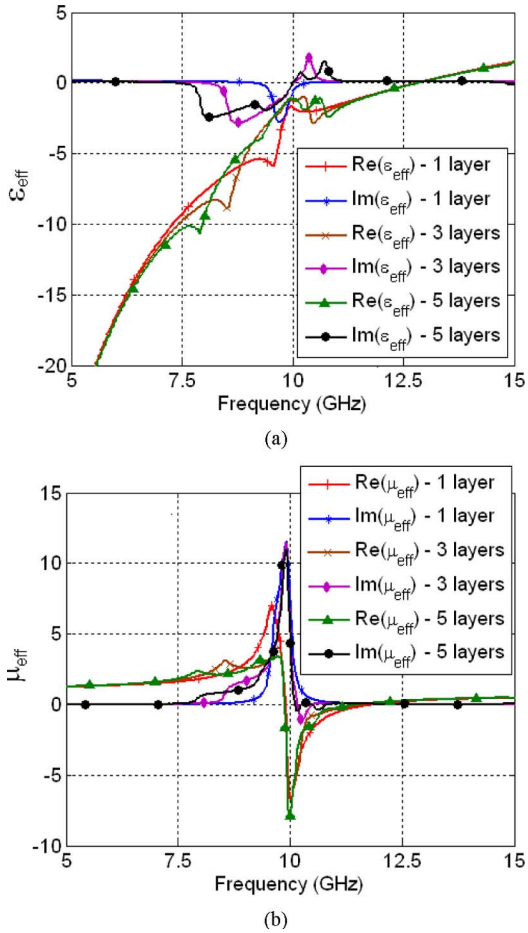

Fig. 10. (a) Electric permittivity and (b) magnetic permeability of one-, three-, and five-unit-cell-thick metamaterial slabs in the first resonant frequency region. Outside of the resonant frequency region, the effective metamaterial parameters are the same for all three cases; however, in the resonant frequency region, they change significantly as a function of the number of layers.

$d_{\text{eff}} = 12.5 \times 10^{-3}$ m and $d_{\text{eff}}/\lambda_{\text{opt}} = 0.76$. As in the previous case, this discontinuity can be interpreted as the upper limit of the effective medium theory. In addition, inspecting the transmission parameter S_{21}, we observe that, at low frequencies, the magnitude is small. The small ripples in the phase of S_{21} are exponentially amplified by (3) and lead to large nonphysical oscillations in the values of the refractive index n_{eff}, noticeable in Fig. 8(a).

Finally, in Fig. 9, an example is presented for which the retrieval algorithm and the effective medium theory cannot predict properly the electromagnetic material parameters. In this case, the metamaterial design contains seven layers of unit cells. This geometry presents challenges for the time-domain electromagnetic field solver because the magnitude of the transmission parameter S_{21} is very small outside the resonant frequency regions. Consequently, due to numerical errors, the phase of S_{21} is not well defined, and this leads to very strong ripples, which will influence the retrieved effective material parameters as well. The ripple greatly affects the real part of the refractive index for the fundamental branch $m = 0$, prohibiting the retrieval of effective material parameters at low frequencies. Checking the continuity of n_{eff} in the resonant frequency region, we observe a discontinuity at $f = 15$ GHz. However, because the oscillating behavior occurs below $f = 10$ GHz, it is difficult to judge the validity of the effective parameters even in the frequency region between 10–15 GHz. The yellow (in online version) and gray areas in Fig. 9(b) represent frequency regions where we cannot extract effective material parameters. The oscillations have a somewhat smaller impact on the imaginary part of the refractive index. Therefore, the refractive index predicted by the Kramers–Kronig relations is relatively smooth and can give an acceptable indication of n_{eff} in the ripple region. In addition, there is a range of frequencies where a good overlap can be found between the refractive index predicted by the Kramers–Kronig formula and the exact values calculated from (4).

Mesh refinements and smaller time steps of the electromagnetic field solver do not eliminate, but reduce the numerical errors in the phase of S_{21}; however, this is not practical because of the resulting increase in the calculation time. This simulation shows the general limitations of the transmission-reflection-based material parameter retrieval techniques.

In Fig. 10, the extracted effective electric permittivity and magnetic permeability of metamaterials, which are one-, three-, and five-unit-cell layers thick, are compared in the frequency range of the first resonance, where the double-negative behavior occurs. As can be observed from Fig. 10, outside of the resonant frequency region, the effective metamaterial parameters are the same for all three cases. Consequently, bulk material properties can be meaningful for describing the metamaterial structures in that frequency range. However, in the resonant frequency region, the electric permittivity and magnetic permeability are changing significantly as a function of the number of layers. This fact demonstrates a long-range electromagnetic coupling between the metamaterial unit cells.

V. Conclusions

We have presented an effective metamaterial parameter retrieval procedure based on Kramers–Kronig relations, demonstrating the applicability, and showing the limits of the algorithm. Our code implementing the presented procedure is published online.[2]

The results obtained with the Kramers–Kronig relations give a suitable approximation for the real part of the refractive index. When the metamaterial is thick (compared to the wavelength), more than one branch is involved in the final result. As the optical thickness becomes comparable to the wavelength, the effective medium theory cannot be applied anymore. The discontinuity of the refractive index indicates that the limit of the effective medium theory has been reached.

When many layers of unit cells are present, the electromagnetic material properties should converge to a bulk value. However, by comparing the retrieved effective metamaterial parameters for different thicknesses, we observe that the effective medium theory breaks down before convergence occurs. This is due to the fact that the geometrical feature sizes are of the order of the wavelength in the frequency range of interest. This

fact invites many questions about the "real material" nature of metamaterials.

ACKNOWLEDGMENT

The authors are grateful to Prof. W. Hoefer, Institute of High Performance Computing, Singapore, for useful technical discussions.

REFERENCES

[1] L. Solymar and E. Shamonina, *Waves in Metamaterials*. Oxford, U.K.: Oxford Univ. Press, 2009.
[2] R. Marqués, F. Martín, and M. Sorolla, *Metamaterials With Negative Parameters*. New York: Wiley, 2008.
[3] C. Krowne and Y. E. Zhang, *Physics of Negative Refraction and Negative Index Materials*. New York: Springer, 2007.
[4] F. Lederer, C. Menzel, and C. Rockstuhl, "Can optical metamaterials be described by effective material parameters?," in *Proc. 3rd Int. Adv. Electromagn. Mater. Microw. Opt. Congr.*, London, U.K., Aug.–Sep. 30–4, 2009, pp. 11–13.
[5] A. M. Nicolson and G. F. Ross, "Measurement of the intrinsic properties of materials by time-domain techniques," *IEEE Trans. Instrum. Meas.*, vol. IM-19, no. 4, pp. 377–382, Nov. 1970.
[6] G. Dolling, C. Enkrich, M. Wegener, C. M. Soukoulis, and S. Linden, "Low-loss negative index metamaterial at telecommunication wavelength," *Opt. Lett.*, vol. 31, pp. 1800–1802, Jun. 2006.
[7] X. Chen, T. M. Grzegorczyk, B. I. Wu, J. Pacheco, and J. A. Kong, "Robust method to retrieve the constitutive effective parameters of metamaterials," *Phys. Rev. E, Stat. Phys. Plasmas Fluids Relat. Interdiscip. Top.*, vol. 70, Feb. 2004, Art. ID 016608.
[8] D. R. Smith, D. C. Vier, T. Koschny, and C. M. Soukoulis, "Electromagnetic parameter retrieval from inhomogeneous metamaterials," *Phys. Rev. E, Stat. Phys. Plasmas Fluids Relat. Interdiscip. Top.*, vol. 71, Mar. 2005, Art. ID 036617.
[9] V. Varadan and R. Ro, "Unique retrieval of complex permittivity and permeability of dispersive materials from reflection and transmitted fields by enforcing causality," *IEEE Trans. Microw. Theory Tech.*, vol. 55, no. 10, pp. 2224–2230, Oct. 2007.
[10] G. Lubkowski, R. Schumann, and T. Weiland, "Extraction of effective material parameters by parameter fitting of dispersive models," *Microw. Opt. Technol. Lett.*, vol. 49, no. 2, pp. 285–288, Jul. 2007.
[11] C. G. Parazzoli, R. B. Greegor, and M. H. Tanielian, "Development of negative index of refraction metamaterials with split ring resonators and wires for RF lens applications," in *Physics of Negative Refraction and Negative Index Materials*, C. Krowne and Y. Zhang, Eds. New York: Springer, 2007, ch. 11, pp. 261–329.
[12] C. Menzel, C. Rockstuhl, T. Paul, F. Lederer, and T. Pertsch, "Retrieving effective parameters for metamaterials at oblique incidence," *Phys. Rev. B, Condens. Matter*, vol. 77, Apr. 2008, Art. ID 195328.
[13] K. Z. Rajab, "Propagation of electromagnetic waves through composite media," Ph.D. dissertation, Dept. Elect. Eng., Pennsylvania State Univ., University Park, PA, 2008.
[14] G. Dolling, M. Wegener, C. M. Soukoulis, and S. Linden, "Negative-index metamaterial at 780 nm wavelength," *Opt. Lett.*, vol. 32, no. 1, pp. 53–55, Jul. 2007.
[15] J. N. Hodgson, *Optical Absorption and Dispersion in Solids*. London, U.K.: Chapman & Hall, 1970.
[16] V. Lucarini, J. J. Saarinen, K. E. Peiponen, and E. M. Vartiainen, *Kramers–Kronig Relations in Optical Materials Research*. Berlin, Germany: Springer-Verlag, 2005.
[17] E. E. Palik, *Handbook of Optical Constants of Solids I–IV*. New York: Academic, 1985–1998.
[18] K. E. Peiponen, V. Lucarini, E. M. Vartiainen, and J. J. Saarinen, "Kramers–Kronig relations and sum rules of negative refractive index media," *Eur. J. Phys. B*, vol. 41, pp. 61–65, Sep. 2004.
[19] P. K. Chattopadhyay, *Mathematical Physics*. New York: Wiley, 1990, pp. 23–24.
[20] G. A. Korn and T. M. Korn, *Mathematical Handbook for Scientists and Engineers*. New York: Dover, 2000.
[21] F. J. Rachford, D. L. Smith, and P. F. Loschialpo, "Experiments and simulations of microwave negative refraction in split ring and wire array negative index materials, 2D split-ring resonator and 2D metallic disk photonic crystals," in *Physics of Negative Refraction and Negative Index Materials*, C. Krowne and Y. Zhang, Eds. New York: Springer, 2007, ch. 9, pp. 217–250.

Zsolt Szabó received the Ph.D. degree in electrical engineering from the Budapest University of Technology and Economics (BME), Budapest, Hungary, in 2002.

From 2001 to 2004, he was Research Engineer with the Tateyama Laboratory Hungary. From 2004 to 2005, he was a Magyary Zoltán Research Fellow with the Department of Atomic Physics, BME. From 2005 to 2007, he was a Japan Society for Promotion of Science Postdoctoral Fellow with the National Institute for Material Science, Tsukuba, Japan. From 2007 to 2009, he was with the National Institute for Nanotechnology, Edmonton, AB, Canada. Since 2009, he has been with the Institute of High Performance Computing, Agency for Science Technology and Research (A*STAR), Singapore, as a Senior Research Engineer. His current research interests include computational electromagnetics, magnetic hysteresis, and composite nanomaterials.

Dr. Szabó is a member of the General Assembly of the Hungarian Academy of Science. He was the recipient of the 2000 Pollák–Virág Award of the Hungarian Telecommunication Scientific Society.

Gi-Ho Park received the B.Sc. degree from Hangyang University, Seoul, Korea, in 1994, the M.Eng. degree in telecommunication from the Asian Institute of Technology, Pathumthani, Thailand, in 1998, and the Ph.D. degree in electrical and computer engineering from the Georgia Institute of Technology, Atlanta, in 2006.

In 2006, he joined the Institute of High Performance Computing, Agency for Science Technology and Research (A*STAR), Singapore, as a Senior Research Engineer. His research interests include computational electromagnetics, metamaterials and photonic crystals.

Ravi Hedge received the B.Eng. degree from the National Institute of Technology, Suratkal, India, in 2001, the M.Sc. degree from the University of Southern California, Los Angeles, in 2002, and the Ph.D. degree from The University of Michigan at Ann Arbor, in 2008, all in electrical engineering.

Since 2009, he has been a Research Engineer with the Institute of High Performance Computing, Agency for Science Technology and Research (A*STAR), Singapore. His research interests include high-frequency metamaterials, plasmonics, and nonlinear fiber optics.

Er-Ping Li (F'08) received the Ph.D. degree in electrical engineering from Sheffield Hallam University, Sheffield, U.K., in 1992.

From 1993 to 1999, he was a Senior Research Fellow, Principal Research Engineer, and the Technical Director with the Singapore Research Institute and Industry. Since 2000, he has been with the Institute of High Performance Computing, Agency for Science Technology and Research (A*STAR), Singapore, where he is currently the Principal Scientist and Director of the Advanced Electronic and Photonics Department. He is also a Guest Professor with Zhejiang University, Hangzhou, China, and a Guest Professor with Peking University, Beijing, China. He has authored or coauthored over 200 papers. He holds a number of U.S. patents. His research interests include computational electromagnetics, microscale/nanoscale integrated circuits and electronic packages, and plasmonic technology.

Dr Li is a Fellow of the Electromagnetics Academy. He was an associate editor for the IEEE MICROWAVE AND WIRELESS COMPONENTS LETTERS from 2006 to 2008. He is currently an associate editor for the IEEE TRANSACTIONS ON ELECTROMAGNETIC COMPATIBILITY. He was the recipient of the Changjiang Chair Professorship Award of the Ministry of Education in China.